Mechanical relaxation of functionalized carbosilane dendrimer melts

Nadezhda N. Sheveleva, Maxim Dolgushev, Erkki Lähderanta, Denis A. Markelov

Mechanical relaxation of functionalized carbosilane dendrimer melts

Nadezhda N. Sheveleva,[1,2]* Maxim Dolgushev,[3†] Erkki Lähderanta,[2]
Denis A. Markelov[1]

[1]*St. Petersburg State University, 7/9 Universitetskaya nab., St. Petersburg, 199034 Russia.*
[2]*Department of Physics, LUT University, Box 20, 53851 Lappeenranta, Finland.*
[3]*Sorbonne Université, CNRS, Laboratoire de Physique Théorique de la Matière Condensée, LPTMC, 4 place Jussieu, 75005 Paris, France.*
*n.n.sheveleva@spbu.ru, †maxim.dolgushev@sorbonne-universite.fr

Abstract

Functionalizing the internal structure of classical dendrimers is a new way of tailoring their properties. Using atomistic molecular dynamics simulations, we investigate the rheological behavior of functionalized dendrimers (FD) melts obtained by modifying the branching of carbosilane dendrimers (CSD). The time (relaxation modulus $G(t)$) and frequency (storage G' and loss G'' moduli) dependencies of the dynamic modulus are obtained. Fourth generation FD melts present a region where $G' > G''$. In contrast, their non-functionalized counterparts (i.e., classical dendrimers with a regular branching) do not show such a region. The comparative analysis of FD and CSD suggests that the internal densification due to functionalization prevents the penetration of branches and causes FD to behave like colloidal particles in a crowded environment. Since CSD have no special interactions, we expect that this effect will be common for other dendrimer macromolecules.

Introduction

Dendrimers are a special class of nano-sized artificial macromolecules with a symmetrical structure, high degree of branching, globular architecture, extremely low polydispersity, and a well-defined molecular weight.[1] Due to their unique structural features and excellent properties, they are widely used as nanocarriers for drug delivery,[2,3] catalysts,[4] nanosensors,[5–7] MRI contrast agents,[8–10] modifiers of rheological properties[11–15] and more. The development of synthesis strategies has led to the appearance of functionalized dendrimers (FD). These compounds form a broad class uniting different dendrimer macromolecules, whose terminal groups, core, and internal repeating units may each or all be modified.[16–18]

Until now dynamical experiments have only been performed on perfectly branching standard dendrimers.[19–25] References[20,21] studied second to fifth generation (denoted G2-G5) polypropyleneimine dendrimers (PPI) at temperatures up to 400 K using NMR relaxometry, dielectric spectroscopy, and rheological methods. Dielectric spectroscopy revealed three relaxation processes in PPI: the main relaxation at melt state temperatures $T > T_g$ and two secondary processes that persist for $T < T_g$, corresponding to the glassy state. The obtained results were compared with those for linear polymers and were found somewhat to be similar to Rouse dynamics. However, a bimodal structure of the relaxation spectrum of G5 PPI dendrimers was revealed, which is not typical for linear chains. The authors suggest that PPI dendrimers are soft enough to allow for partial interpenetration, which decreases with increasing generation. Other compounds like carbosilane dendrimers (CSD) [26–28] in condensed state (bulk or melt) have been studied in the Refs.[22–25] A sharp increase in viscosity (or "jump") in viscosity in CSD melts was observed high for generations ($G > 5$).[22] Moreover similar behavior was observed for approximately 40% of G5 PPI dendrimers at 493 K by NMR spectroscopy.[24] The authors suggested that this effect is due to the dendrimer network, which is formed via physical entanglements, however this hypothesis has not yet been confirmed. Thus, the nature of this dendrimer network is not clear.

In a recent work[29] by some of us, rheological properties of G2-G4 CSD melts were studied by molecular dynamics (MD) simulations. The method[30] used allows the study classical polymer melts, but not polymer networks like those experimentally observed for G5 CSD; hence we were limited to G4 CSD. The study has confirmed the presence of different relaxation processes predicted by the theory describing a single macromolecule.[31–36] Thereby the oversimplified elastic ball description of dendrimers is rejected in the appropriate time/frequency range of the dynamic modulus. For all G2-G4 CSD melts, effects of network formation were not observed. Meanwhile, signs of intermolecular interactions were found for G4, which manifest through the melt's maximal mechanical relaxation time being longer than for an individual dendrimer.

Herein we consider functionalized CSD dendrimers (FD) containing non-branching aliphatic segments beginning from branching points (see Fig.1). We will show by MD simulations at atomistic resolution that a slight change in its topological structure (the introduction of additional segments into the interior of the classical CSD) is sufficient to cause a characteristic slowdown in mechanical relaxation of higher

generation dendrimers. The analysis of static and dynamic properties suggests that this behavior can be associated with decreasing interpenetration effects. The dendrimers become closer to colloidal particles that are progressively restricted in translational motion.

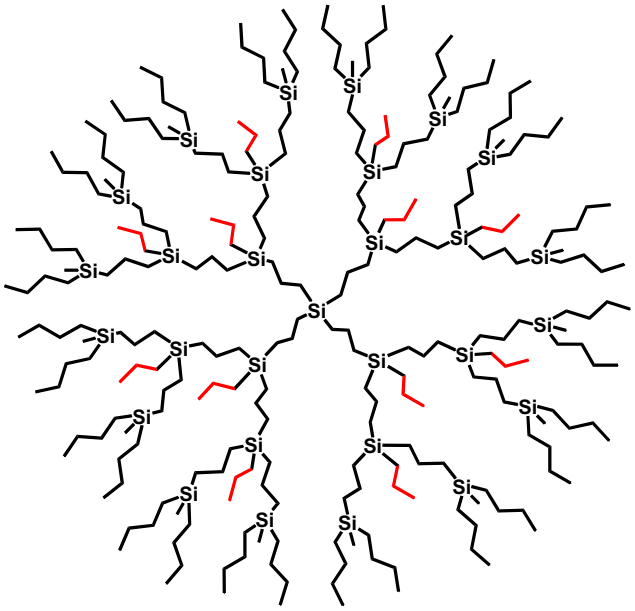

Figure 1. Structure of a functionalized second generation carbosilane dendrimer (G2 FD). The difference between FD and carbosilane dendrimers (CSD) is highlighted in red (for CSD, the red segments are absent).

Methods

Mechanical relaxation is studied by adapting the method used in Ref.[29] In the Electronic Supplementary Information (ESI), we recall it briefly and provide the relevant information for this study. The method overcomes the difficulty of covering the huge time scale differences inherent to mechanical relaxation. Its main feature is the superposition of relaxation curves obtained for dynamical systems subject to various internal frictions (controlled by the Langevin thermostat maintaining the systems at 600 K). The dynamical modulus $G(t)$ is calculated from fluctuations of the stress tensor $\widehat{\mathbf{P}} = (P_{\alpha\beta})$:[37,38]

$$G(t) = \frac{V}{30k_{\mathrm{B}}\mathrm{T}}\sum_{(\alpha\beta)}(6\langle P_{\alpha\beta}(t)P_{\alpha\beta}(0)\rangle + \langle N_{\alpha\beta}(t)N_{\alpha\beta}(0)\rangle). \quad (1)$$

Here V is the box volume, T is the temperature, k_{B} is the Boltzmann constant, $N_{\alpha\beta} = P_{\alpha\alpha} - P_{\beta\beta}$, where $(\alpha\beta)$ sums over the xy, yz, zx components of $\widehat{\mathbf{P}} = (P_{\alpha\beta})$.

Results

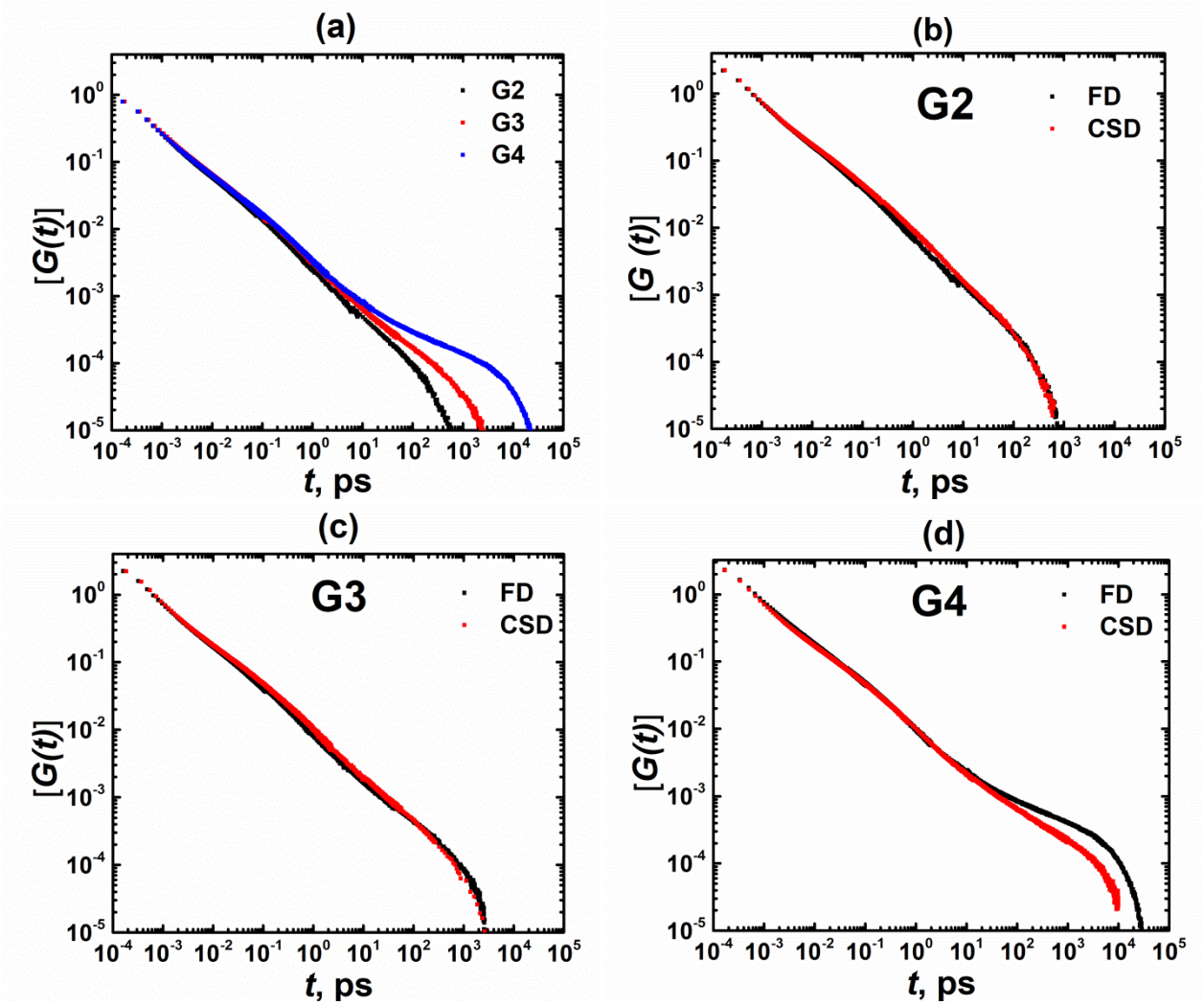

Figure 2. Double-logarithmic representation of the normalized shear-stress relaxation modulus $[G(t)] \equiv G(t)/G(0)$ of melts of (a) FD at generation G2-G4; (b)-(d) of FD (black) and CSD (red) plotted separately for each generation.

Figure 2(a) illustrates $G(t)$ of FD at different generations. At short times the curves superimpose for different generations, revealing universal behavior for all FD. This region could be associated with the tension relaxation,[29] in analogy with Refs.[31,39,40] At intermediate times (0.1 to 5ps), one observes little variations between generations. For standard dendrimers of different generations, e.g., for CSD, there are no differences in this time interval,[29] as for shorter times. We note that this time region depends on the internal relaxation modes, which are independent of the dendrimer's size.[33,41] However, in the case of FD, an additional process related to the irregular branching appears in that intermediate region. Though the corresponding relaxation times only insignificantly depend on generation, the contribution of this additional process might be different. In order to examine this observation, Fig. 2(b)-(d) directly compares $G(t)$ of FD and CSD. The figure shows no differences between G4 FD and G4 CSD at short and intermediate times. Meanwhile, $G(t)$ for FD of lower generations is

located slightly under that of CSD; the effect is strongest at the smallest generation. Hence one can infer that the contribution of this specific process (FD process) decreases with growing generation. Note that, notwithstanding this FD process being barely detectable in mechanical relaxation experiments, its presence is significant for dielectric[42] and NMR[43] relaxations. Particularly, we established that the FD process appears in NMR relaxation of CSD melts.[43] It turns out that one chemical bond appearing at each branching point (see Fig. 1) in CSD is enough for the manifestation of the FD process in the NMR relaxation at the intermediate times (albeit not affecting the longer times[42,43]).

Table 1. The time τ_{max} characterizing the tail of the relaxation modulus of FD ($G(t) \propto \exp(-2t/\tau_{max})$) and the time τ_{rot} characterizing the rotation of FD as a whole. For comparison, the same values for the CSD dendrimers obtained in work[29] are shown. All data are given for the parameter τ_T = 0.5 ps of the Langevin thermostat, see SI for details.

G	FD					CSD				
	R_g, nm	τ_{rot}, ns	τ_{max}, ns	τ_{rot}/R_g^3, ns/nm^3	τ_{max}/τ_{rot}	R_g, nm	τ_{rot}, ns	τ_{max}, ns	τ_{rot}/R_g^3, ns/nm^3	τ_{max}/τ_{rot}
2	0.874	0.685	0.470	1.03	0.69	0.872	0.831	0.461	1.25	0.55
3	1.141	2.56	2.24	1.73	0.88	1.119	2.83	1.98	2.01	0.7
4	1.441	8.03	16.8	2.69	2.09	1.394	7.03	9.6	2.62	1.36

At longer times, one observes the region characterized through overall branch relaxation. As for CSD, this process depends on the size of the dendrimers' branches. Therefore, also in the case of FD, increasing generation leads to slower relaxation, see Fig. 2(a). Comparing both FD and CSD for G2 and G3 in Fig. 2(b)-(c) shows a practical coincidence. Meanwhile, for G4, Fig. 2(d) shows $G(t)$ for FD decaying slower than for CSD. One might think that this effect is related to the higher molecular mass of FD branches, given that the corresponding relaxation times depend on it.[33,41] However, the huge slowdown effect cannot be attributed to branch relaxation. In our previous study of CSD, a similar but much less pronounced effect has also been observed.[29] We have shown that the exponential tail of $G(t)$ (i.e. the terminal region, where $G(t) \propto \exp(-2t/\tau_{max})$) is characterized by the time τ_{max}, which is longer than the rotational relaxation time τ_{rot} (defined from the rotational autocorrelation function in SI) for G4, whereas it is shorter for lower generations. Given that the time τ_{rot} is the maximal relaxation time of a single dendrimer, this effect shows that there are important interactions between the dendrimers. Looking at the τ_{max} for FD, the effect turns out to be much more dramatic, see Table 1. We will consider the reasons for this fact in the section “Discussion”.

Based on $G(t)$, we can calculate experimentally relevant storage $G'(\omega)$ and loss $G''(\omega)$ moduli using the Fourier transform, $G'(\omega) + iG''(\omega) = i\omega\int G(t)\exp(-i\omega t)dt$.[44] The result is presented on Fig. 3(a)-(b). As expected, at high frequencies both $G'(\omega)$ and $G''(\omega)$ do not depend on the size of FD. At very low frequencies, we find the expected behavior $G'(\omega) \propto \omega^2$ and $G''(\omega) \propto \omega$.[44] The crossover to this behavior is determined by

the time τ_{max} that strongly depends on the dendrimers' size. The greater the dendrimers' generation, the lower the frequency at which the moduli reach the terminal regime.

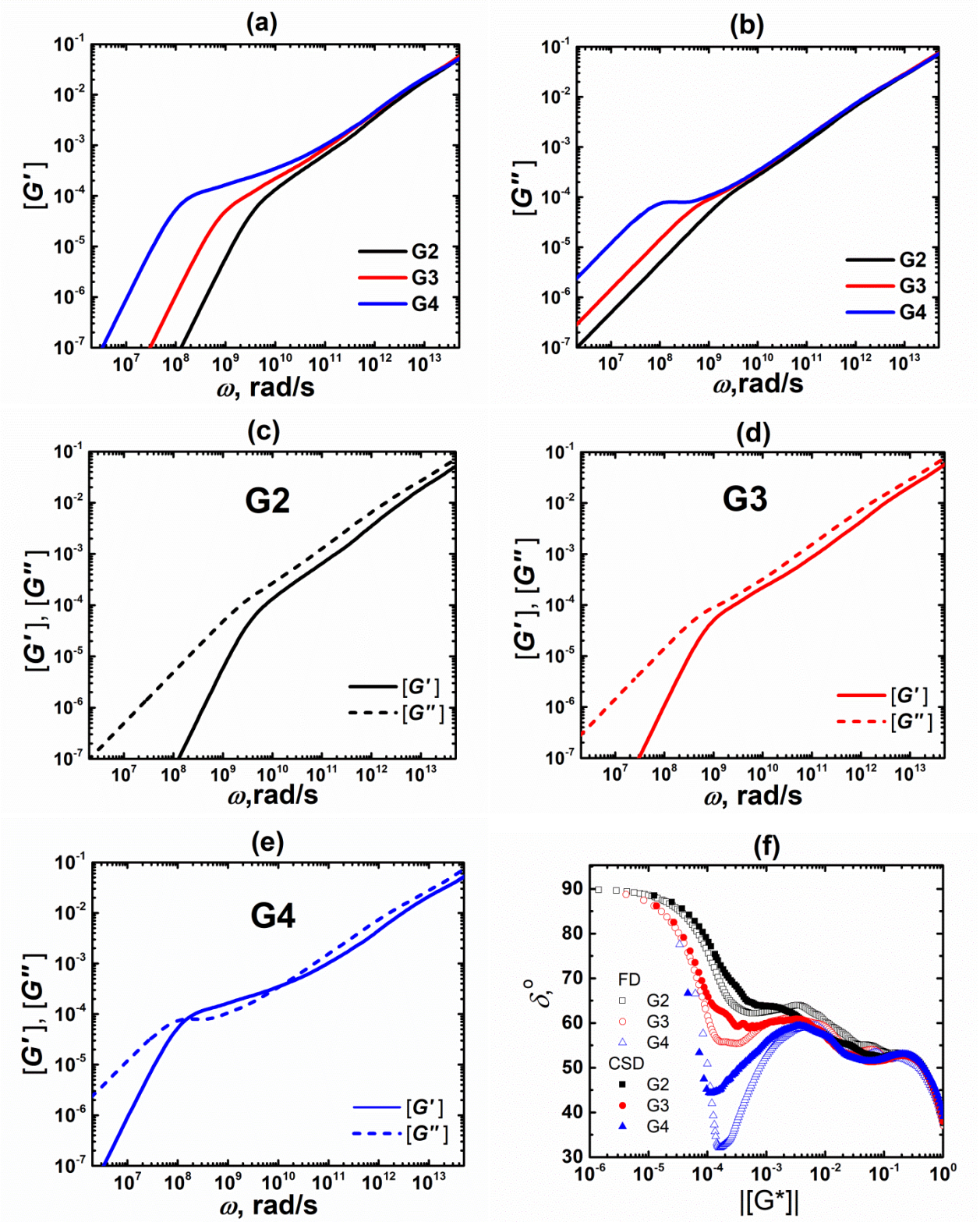

Figure 3. Double-logarithmic representation of the storage $[G'(\omega)]$ and loss $[G''(\omega)]$ moduli for FD melts; (a)-(b) the moduli for G2, G3, and G4; (c)-(e) $[G'(\omega)]$ and $[G''(\omega)]$ plotted together, separately for each generation; (f) the Booij−Palmen plot (Eq. (2)) for FD and CSD melts of G2-G4.

In the intermediate frequency region, one observes different features of mechanical relaxation between generations. In particular, Fig.3(c)-(e) displays G' and G'' for each generation, where qualitative differences between G2, G3 and G4 are immediately apparent. While for lower generations $G' < G''$, for G4 at lower intermediate frequencies a region is found spanning almost two orders of frequencies, where $G' > G''$. Note that for CSD, G' and G'' do not intersect each other even for G4.[29] The next section analyzes the reasons for the different behavior of G4 FD and G4 CSD, appearing despite the slight difference in structure.

Discussion

Aiming to quantify the effects in dendrimer systems, we begin by considering the Booij−Palmen plots,[45] see Fig. 3(f). In this representation, the dependence of the phase angle:

$$\delta(|G^*|) = \arctan\left(\frac{G''}{G'}\right) \tag{2}$$

on the absolute value of the complex dynamic modulus $|G^*| = \sqrt{G'^2 + G''^2}$ is analyzed. The values of δ close to 90° are related to the terminal flow region. The glassy state of a polymeric system manifests itself at $\delta \to 0$. Figure 3(f) displays δ vs $|G^*|$ for FD and CSD of G2, G3, and G4. As can be inferred from the figure, the phase angle is $\delta > 45°$ for both FD and CSD of G2 and G3, for G4 CSD the minimal value of the phase angle is $\delta_{\min} \approx 45°$; only for G4 FD, the phase angle δ approaches 30°. We note that similar minimal values of δ are observed experimentally for hyperbranched polyglycerol (hbPG) melts of high molecular mass.[46] At the same time, such a minimum was absent for weights $M_{\text{hbPG}} < 10000$ g/mol. In the work,[46] the authors explain the deep minimum below $\delta < 45°$ (i.e., $G' > G''$) by the presence of entanglements, as for melts of linear chains, for which $\delta < 45°$ is usually related to a rubbery plateau.[44,46] Furthermore, we will show that in the case of dendrimer melts, the slowdown corresponding to $\delta < 45°$ is of different nature (maybe because of very different structure of hbPG, whose large-scale behavior is more polymeric in comparison with the dendrimers). Here, we have an excellent opportunity to compare two different dendrimer melts (consisting of macromolecules with similar radii of gyration, see Table 1), in one of them the slowdown effects are barely present (CSD, for which $\delta_{\min} \approx 45°$) and in the other they are clearly manifested (FD, for which $\delta_{\min} \approx 30°$).

It is natural to suppose that the slowdown affects the translational mobility of dendrimers. For its analysis we consider in Figure 4 the mean-square displacement of dendrimer's centers of mass:

$$MSD(t) = < (\vec{r}_{cm}(t_0 + t) - \vec{r}_{cm}(t_0))^2 >_{t_0} \tag{3}$$

where $\vec{r}_{cm}(t)$ is the vector of the position of the center of mass of the dendrimer at the time t; averaged over initial instants of time t_0. As can be seen in Figure 4, there is a region of anomalous diffusion that is more pronounced for FD G4. By looking at the derivative of the curves, d ln(MSD)/d ln(t), we observe a minimum that deepens and

broadens with functionalization and generation. We conclude that indeed the translational mobility of dendrimers diminishes with growing molecular mass.

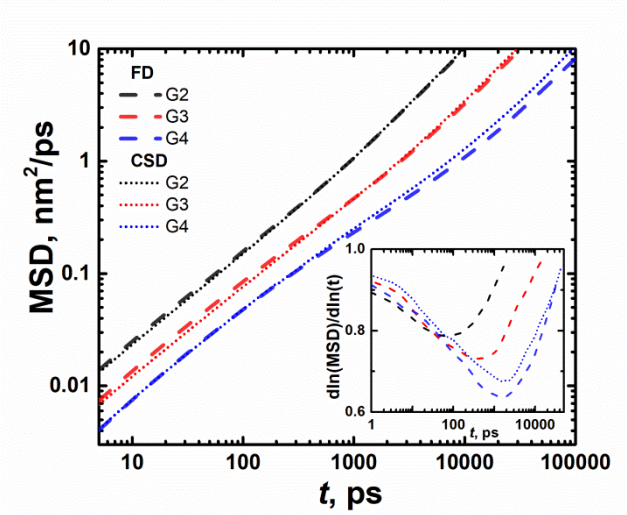

Figure 4. Mean square displacement (MSD) of center-of-masses of FD and CSD. Inset: Derivatives of a double logarithmic function of MSD for the same macromolecules.

For understanding of nature of slowdown effect and anomalous diffusion we start by examining the equilibrium properties of FD and CSD melts. First, the polymeric behavior is associated with an increase in the mutual penetration of macromolecules.[47,48] We start by looking at the radial distribution function (RDF) of the dendrimers' centers of mass, see Fig. 5. The RDF becomes sharper with functionalization and with generation. This shows that the penetration between different dendrimers decreases.

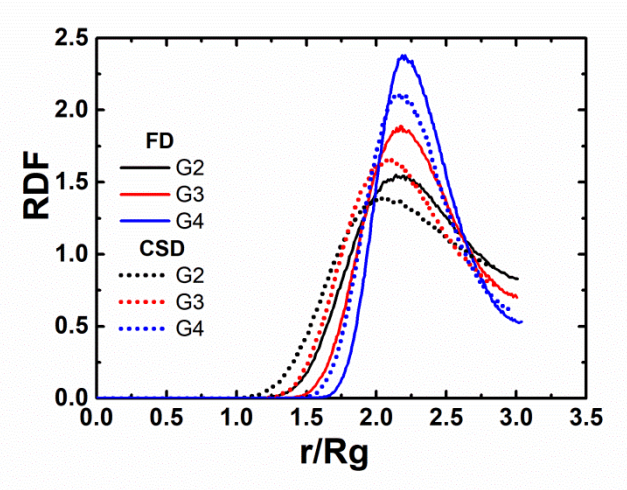

Figure 5. Radial distribution function (RDF) for distance r between the center-of-mass of FD and CSD, as a function of r/R_g, where R_g is radius of gyration of a macromolecule.

To estimate the degree of penetration, we calculate the radial density profiles from the center of mass of the macromolecule both for one dendrimer, ρ_D, and for the rest of the dendrimers in the system, $\rho_{overlap}$, using the formula:

$$\rho(r) = \frac{< m(r) >}{V(r)} \tag{4}$$

where $\rho(r)$ is the average density in the spherical layer at a distance r from the dendrimer's center of mass, $<m(r)>$ is the average total mass of atoms in the layer of volume $V(r)$. The obtained curves are shown in Figure 6. As can be seen from Figure 6(a), in the inner region ρ_D weakly depends on the dendrimer's generation. However, the density of FD is higher than that of CSD. Moreover, Figure 6(b) shows that the mutual penetration of dendrimers is less for G4 FD than for G4 CSD: the $\rho_{overlap}$ curve for FD is shifts towards greater r, which should prevent the interpenetration.

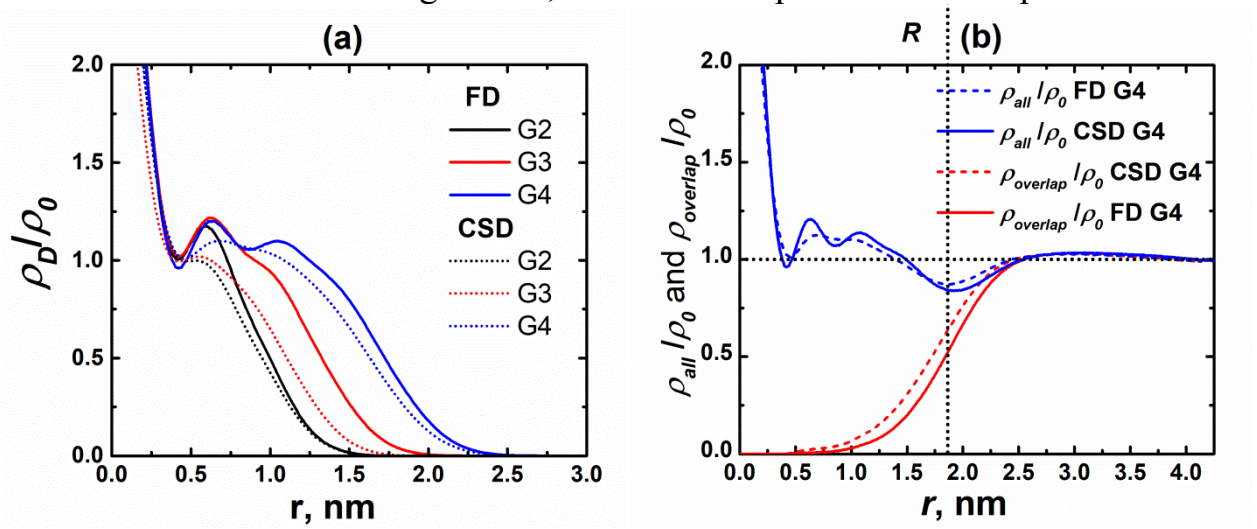

Figure 6. The radial density distribution functions for (a) the selected dendrimer, ρ_D, (b) all dendrimers, ρ_{all}, and all dendrimers without the selected dendrimer, $\rho_{overlap}$, calculated from the center of mass of the individual dendrimer. The horizontal dashed line corresponds to the average density of melts; the vertical dashed line indicates $R = \sqrt{5/3}R_g$ of G4 FD.

For a more quantitative illustration of the degree of mutual penetration of dendrimers, we consider

$$J_{overlap} = \frac{M_{over}}{M_D}, \quad (5)$$

where M_{over} is the molecular weight of atoms of neighboring dendrimers within a radius of $R = \sqrt{5/3}R_g$ from the center of mass of the chosen dendrimer and M_D is the molecular weight of the dendrimer. $J_{overlap}$ for CSD and FD of different generations are shown in Figure 7. The penetration degree of CSD is at least 1.5 times higher than that of FD. Thus, FD dendrimers have a denser structure and, as a consequence, a lower degree of penetration. Therefore, the possibility of polymeric interpenetration decreases with the functionalization of dendrimers, as well as with an increase in generation.

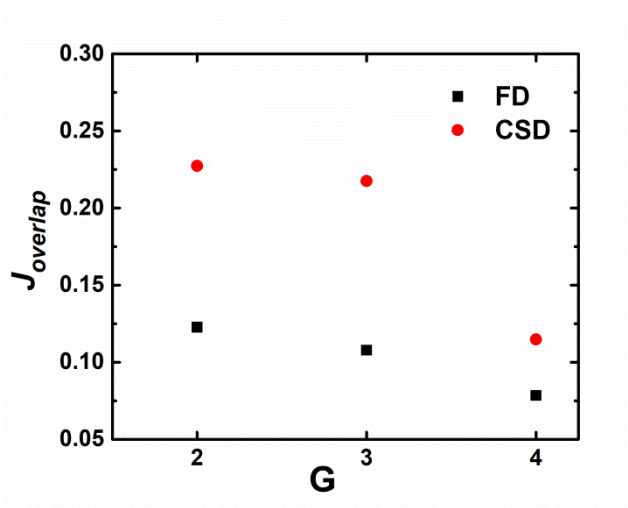

Figure 7. The penetration degree $J_{overlap}$ defined by Eq. (5) for FD and CSD at different generations.

From a dynamics perspective, interpenetrations significantly slow down the rotation of the dendrimer as a whole. In this respect, it is convenient to look at the characteristic time of this rotation, τ_{rot}. However, in order to compare the τ_{rot} values for dendrimers of different molecular weights, it is necessary to account their difference in size, which can be quantified through R_g (or the hydrodynamic radius R_h proportional to it). Then one expects[49] that the parameter

$$\boldsymbol{B} = \tau_{rot} / R_g^3 \qquad (6)$$

is independent of dendrimers' size. As can be inferred from Table 1, this parameter is smaller than 2 ns/nm^3 for G2 and G3 of FD and CSD and around 2.6 ~ 2.7 ns/nm^3 for G4, which is almost the same for FD and CSD. Thus, $\boldsymbol{B}$ is insensitive to the slowdown of mechanical relaxation and, therefore, does not confirm the interpenetrations between dendrimers.

Now, as we have shown above, FD becomes similar to an impenetrable nanoparticle. Therefore, it is reasonable to assume that the slowdown of mechanical relaxation occurs due to the transition from polymeric to colloidal behavior as it has also recently been discovered for multiarm star polymers with dendrimer cores.[47,48] We assume that this effect is common for other dendrimer macromolecules. In particular, for carbosilane dendrimers, this is in line with the following observations:
(i) MD simulations of CSD melts of different generations (G = 2-8) showed an increase in free volume between CSD dendrimers with an increase in the dendrimer size.[50]
(ii) A sharp increase in the viscosity of CSD melts from G4 to G6 was also found.[22]
(iii) Moreover, the G6 CSD melt exhibits crystalline properties observed in the SAXS experiment.[23] Apparently, this effect is similar to the ordering of hard spheres.[51]
It can be assumed that the very strong slowdown effects begin to manifest themselves for CSD for $G \geq 5$ that makes difficult to use our method for investigation of such systems. Thus, additional "tuning" of G4 CSD due to functionalization allows us to observe such effects in the dendrimer melts on mechanical relaxation.

Finally, we consider the terminal time of mechanical relaxation, τ_{max}. For G2 and G3, FD and CSD take similar values of τ_{max} and τ_{rot}. A completely different tendency is observed for G4: τ_{max} becomes almost two times longer for FD in comparison to CSD.

We can conclude that τ_{max} is more sensitive to the transition between polymeric and colloidal behavior than τ_{rot}. Since τ_{rot} is only determined by the dendrimer's size, Table 1 therefore uses the ratio τ_{max}/τ_{rot} to eliminate the size contribution from τ_{max}. This ratio is lower than 1 for the systems in which the low-frequency behavior of the mechanical relaxation modulus is determined by the relaxation time of the dendrimer's largest branch, which is shorter than the rotational relaxation time τ_{rot}.[52,53] The presence of strong intermolecular interactions leads to $\tau_{max} > \tau_{rot}$. Table 1 shows that for both FD and CSD of G4, $\tau_{max}/\tau_{rot} > 1$, but for FD this ratio is much higher (2.09 for FD vs 1.39 for CSD).

Conclusions

This work investigated the rheological properties of functionalized carbosilane dendrimers (FD) using atomistic molecular dynamics simulations. The results were compared with those previously obtained by us for standard carbosilane dendrimers (CSD) of the same chemistry and similar molecular mass. The minimal difference between the structures (see Fig. 1) leads to the significant slowdown of mechanical relaxation of FD melts compared to corresponding CSD melts especially for high enough generations. For example, the terminal relaxation time, $\tau_{max,}$ is 1.75 times greater for G4 FD than for G4 CSD. This slowdown of mechanical relaxation leads to an appearance of a region spanning almost two orders of frequencies where the storage modulus G' is larger than the loss modulus G''. As a consequence, we find a sharp minimum in arctan(G''/G') for G4 FD. Comparative analysis of static properties shows that functionalization leads to the densification of the dendrimers, which, consequently, penetrate each other less; and so progressively resembling a colloidal system of impenetrable nanoparticles in a crowded environment. This is in line with the comparison between the longest characteristic times appearing in the rotational mobility (τ_{rot}) and in the mechanical relaxation (τ_{max}). It was established that the rotational mobility of the dendrimer as a whole is not sensitive to the slowdown of mechanical relaxation. While the change of rotational motion can only be attributed to the change of the size of individual dendrimers, the mechanical relaxation clearly indicates significant interactions between the macromolecules. Since interpenetrations could cause collective rotations and therefore affect considerably the rotational motion, the MSD of the dendrimers' centers of mass indicates that the slowdown is caused by restrictions on the translational motion. In this way, the ratio τ_{max}/τ_{rot} can serve as a criterion for the manifestation of this effect. We suggest that the effect found for carbosilane-type dendrimers is common for other dendrimer macromolecules.

Conflicts of interest

There are no conflicts to declare.

Acknowledgments

The simulations were performed in Computer Science Center (CSC) of Finland and in Computer Resources Center of Saint Petersburg State University. N.N.S. is supported by the Russian Science Foundation (No. 21-73-00067). E.L. and D.A.M. are thankful for the Researcher Mobility Grant of the Academy of Finland (No. 334244). N.N.S. is thankful for the travel grant provided by Saint Petersburg State University (Event 6, ID 48528925).

References

1 M. A. Mintzer and M. W. Grinstaff, Biomedical applications of dendrimers: a tutorial, *Chem. Soc. Rev.*, 2011, **40**, 173–190.

2 J. Yang, Q. Zhang, H. Chang and Y. Cheng, Surface-Engineered Dendrimers in Gene Delivery, *Chem. Rev.*, 2015, **115**, 5274–5300.

3 R. Sapra, R. P. Verma, G. P. Maurya, S. Dhawan, J. Babu and V. Haridas, Designer Peptide and Protein Dendrimers: A Cross-Sectional Analysis, *Chem. Rev.*, 2019, **119**, 11391–11441.

4 K. Yamamoto, T. Imaoka, M. Tanabe and T. Kambe, New Horizon of Nanoparticle and Cluster Catalysis with Dendrimers, *Chem. Rev.*, 2020, **120**, 1397–1437.

5 R. Walsh, J. M. Morales, C. G. Skipwith, T. T. Ruckh and H. A. Clark, Enzyme-linked DNA dendrimer nanosensors for acetylcholine, *Sci. Rep.*, 2015, **5**, 14832.

6 A. Shakhbazau, M. Mishra, T.-H. Chu, C. Brideau, K. Cummins, S. Tsutsui, D. Shcharbin, J.-P. Majoral, S. Mignani, M. Blanchard-Desce, M. Bryszewska, V. W. Yong, P. K. Stys and J. van Minnen, Fluorescent Phosphorus Dendrimer as a Spectral Nanosensor for Macrophage Polarization and Fate Tracking in Spinal Cord Injury, *Macromol. Biosci.*, 2015, **15**, 1523–1534.

7 C. M. Lamy, O. Sallin, C. Loussert and J.-Y. Chatton, Sodium Sensing in Neurons with a Dendrimer-Based Nanoprobe, *ACS Nano*, 2012, **6**, 1176–1187.

8 J. Zhu, E. M. Gale, I. Atanasova, T. A. Rietz and P. Caravan, Hexameric Mn II Dendrimer as MRI Contrast Agent, *Chem. - A Eur. J.*, 2014, **20**, 14507–14513.

9 W. Yu, Y. Yang, S. Bo, Y. Li, S. Chen, Z. Yang, X. Zheng, Z.-X. Jiang and X. Zhou, Design and Synthesis of Fluorinated Dendrimers for Sensitive 19 F MRI, *J. Org. Chem.*, 2015, **80**, 4443–4449.

10 A. C. Opina, K. J. Wong, G. L. Griffiths, B. I. Turkbey, M. Bernardo, T. Nakajima, H. Kobayashi, P. L. Choyke and O. Vasalatiy, Preparation and long-term biodistribution studies of a PAMAM dendrimer G5–Gd-BnDOTA conjugate for lymphatic imaging, *Nanomedicine*, 2015, **10**, 1423–1437.

11 T. Kuang, L. Chang, D. Fu, J. Yang, M. Zhong, F. Chen and X. Peng, Improved crystallizability and processability of ultra high molecular weight polyethylene modified by poly(amido amine) dendrimers, *Polym. Eng. Sci.*, 2017, **57**, 153–160.

12 L. Shi, C. Liu, M. Chen, Z. Hua, Z. Ye and J. Zhang, Synthesis and evaluation of a hyperbranched copolymer as viscosity reducer for offshore heavy oil, *J. Pet. Sci. Eng.*, 2021, **196**, 108011.

13 H. Zhao, B. Liao, F. Nian, Y. Zhao, K. Wang and H. Pang, Synthesis and characterization of a PAMAM dendrimer-based superplasticizer and its effect on the properties in cementitious system, *J. Appl. Polym. Sci.*, 2018, **135**, 1–11.

14 D. Kang and H. Kim, Improvement in nano-pattern replication of injection molding by polyamide/dendrimer blend, *Polym. Eng. Sci.*, 2021, **61**, 822–829.

15 M. Wengenmayr, R. Dockhorn and J. U. Sommer, Dendrimers in Solution of Linear Polymers: Crowding Effects, *Macromolecules*, 2019, **52**, 2616–2626.

16 M. Sowinska and Z. Urbanczyk-Lipkowska, Advances in the chemistry of

dendrimers, *New J. Chem.*, 2014, **38**, 2168.
17 T. Kang, R. J. Amir, A. Khan, K. Ohshimizu, J. N. Hunt, K. Sivanandan, M. I. Montañez, M. Malkoch, M. Ueda and C. J. Hawker, Facile access to internally functionalized dendrimers through efficient and orthogonal click reactions, *Chem. Commun.*, 2010, **46**, 1556–1558.
18 S. Hecht, Functionalizing the interior of dendrimers: Synthetic challenges and applications, *J. Polym. Sci. Part A Polym. Chem.*, 2003, **41**, 1047–1058.
19 S. Uppuluri, F. A. Morrison and P. R. Dvornic, Rheology of dendrimers. 2. Bulk polyamidoamine dendrimers under steady shear, creep, and dynamic oscillatory shear, *Macromolecules*, 2000, **33**, 2551–2560.
20 F. Mohamed, M. Hofmann, B. Pötzschner, N. Fatkullin and E. A. Rössler, Dynamics of PPI Dendrimers: A Study by Dielectric and H-2 NMR Spectroscopy and by Field-Cycling H-1 NMR Relaxometry, *Macromolecules*, 2015, **48**, 3294–3302.
21 M. Hofmann, C. Gainaru, B. Cetinkaya, R. Valiullin, N. Fatkullin and E. A. Rössler, Field-Cycling Relaxometry as a Molecular Rheology Technique: Common Analysis of NMR, Shear Modulus and Dielectric Loss Data of Polymers vs Dendrimers, *Macromolecules*, 2015, **48**, 7521–7534.
22 V. G. Vasil'ev, E. Y. Kramarenko, E. A. Tatarinova, S. A. Milenin, A. A. Kalinina, V. S. Papkov and A. M. Muzafarov, An unprecedented jump in the viscosity of high-generation carbosilane dendrimer melts, *Polymer (Guildf).*, 2018, **146**, 1–5.
23 A. V. Bakirov, E. A. Tatarinova, S. A. Milenin, M. A. Shcherbina, A. M. Muzafarov and S. N. Chvalun, Close-packed polybutylcarbosilane dendrimers of higher generations, *Soft Matter*, 2018, **14**, 9755–9759.
24 V. V Matveev, D. A. Markelov, S. V Dvinskikh, A. N. Shishkin, K. V Tyutyukin, A. V Penkova, E. A. Tatarinova, G. M. Ignat'eva and S. A. Milenin, Investigation of Melts of Polybutylcarbosilane Dendrimers by 1H NMR Spectroscopy, *Sci. Rep.*, 2017, **7**, 13710.
25 K. Boldyrev, A. Chernyak, I. Meshkov, A. Muzafarov, E. Tatarinova and S. Vasil'ev, The self-diffusion of polymethylsilsesquioxane (PMSSO) dendrimers in diluted solutions and melts, *Soft Matter*, , DOI:10.1039/d0sm01183e.
26 E. A. Tatarinova, E. A. Rebrov, V. D. Myakushev, I. B. Meshkov, N. V. Demchenko, A. V. Bystrova, O. V. Lebedeva and A. M. Muzafarov, Synthesis and study of the properties of the homologous series of polyallylcarbosilane dendrimers and their nonfunctional analogs, *Russ. Chem. Bull.*, 2004, **53**, 2591–2600.
27 L. L. Zhou and J. Roovers, Synthesis of novel carbosilane dendritic macromolecules, *Macromolecules*, 1993, **26**, 963–968.
28 J. Roovers and J. Ding, in *Silicon-Containing Dendritic Polymers*, Springer Netherlands, Dordrecht, 2009, pp. 31–74.
29 M. Dolgushev, D. A. Markelov and E. Lähderanta, Linear Viscoelasticity of Carbosilane Dendrimer Melts, *Macromolecules*, 2019, **52**, 2542–2547.
30 A. E. Likhtman, S. K. Sukumaran and J. Ramirez, Linear Viscoelasticity from

Molecular Dynamics Simulation of Entangled Polymers, *Macromolecules*, 2007, **40**, 6748–6757.
31 D. C. Morse, Viscoelasticity of Concentrated Isotropic Solutions of Semiflexible Polymers. 2. Linear Response, *Macromolecules*, 1998, **31**, 7044–7067.
32 C. Cai and Z. Y. Chen, Rouse Dynamics of a Dendrimer Model in the ϑ Condition, *Macromolecules*, 1997, **30**, 5104–5117.
33 Y. Y. Gotlib and D. A. Markelov, Theory of the Relaxation Spectrum of a Dendrimer Macromolecule, *Polym. Sci. Ser. A*, 2002, **44**, 1341–1350.
34 Y. Y. Gotlib and D. A. Markelov, Theory of orientational relaxation of individual specified units in a dendrimer, *Polym. Sci. Ser. A*, 2007, **49**, 1137–1154.
35 P. Biswas, R. Kant and A. Blumen, Polymer dynamics and topology: Extension of stars and dendrimers in external fields, *Macromol. Theory Simulations*, 2000, **9**, 56–67.
36 M. Dolgushev and A. Blumen, Dynamics of semiflexible chains, stars, and dendrimers, *Macromolecules*, 2009, **42**, 5378–5387.
37 J. Ramírez, S. K. Sukumaran, B. Vorselaars and A. E. Likhtman, Efficient on the fly calculation of time correlation functions in computer simulations, *J. Chem. Phys.*, 2010, **133**, 154103.
38 A. David, A. De Nicola, U. Tartaglino, G. Milano and G. Raos, Viscoelasticity of Short Polymer Liquids from Atomistic Simulations, *J. Electrochem. Soc.*, 2019, **166**, B3246–B3256.
39 R. Granek, From Semi-Flexible Polymers to Membranes: Anomalous Diffusion and Reptation, *J. Phys. II*, 1997, **7**, 1761–1788.
40 C. P. Broedersz and F. C. MacKintosh, Modeling semiflexible polymer networks, *Rev. Mod. Phys.*, 2014, **86**, 995–1036.
41 D. A. Markelov, M. Dolgushev, Y. Y. Gotlib and A. Blumen, NMR relaxation of the orientation of single segments in semiflexible dendrimers, *J. Chem. Phys.*, 2014, **140**, 244904.
42 J. Grimm and M. Dolgushev, Dynamics of internally functionalized dendrimers, *Phys. Chem. Chem. Phys.*, 2016, **18**, 19050–19061.
43 N. N. Sheveleva, M. Dolgushev, E. Lähderanta and D. A. Markelov, NMR Relaxation of Functionalized Dendrimers, *Macromolecules*, 2019, **52**, 9766–9772.
44 J. D. Ferry, *Viscoelastic properties of polymers*, 1980.
45 H. C. Booij and J. H. M. Palmen, Some aspects of linear and nonlinear viscoelastic behaviour of polymer melts in shear, *Rheol. Acta*, 1982, **21**, 376–387.
46 C. Schubert, C. Osterwinter, C. Tonhauser, M. Schömer, D. Wilms, H. Frey and C. Friedrich, Can hyperbranched polymers entangle? Effect of hydrogen bonding on entanglement transition and thermorheological properties of hyperbranched polyglycerol melts, *Macromolecules*, 2016, **49**, 8722–8737.
47 D. Vlassopoulos and M. Cloitre, Tunable rheology of dense soft deformable colloids, *Curr. Opin. Colloid Interface Sci.*, 2014, **19**, 561–574.
48 L. Gury, M. Gauthier, M. Cloitre and D. Vlassopoulos, Colloidal Jamming in Multiarm Star Polymer Melts, *Macromolecules*, 2019, **52**, 4617–4623.
49 V. N. N. Tsvetkov, Structure and properties of rigid chain polymer molecules in

solutions, *Polym. Sci. U.S.S.R.*, 1979, **21**, 2879–2899.
50 N. K. Balabaev, M. A. Mazo and E. Y. Kramarenko, Insight into the Structure of Polybutylcarbosilane Dendrimer Melts via Extensive Molecular Dynamics Simulations, *Macromolecules*, 2017, **50**, 432–445.
51 M. H. Yamani and M. Oettel, Stable and metastable hard-sphere crystals in fundamental measure theory, *Phys. Rev. E*, 2013, **88**, 22301.
52 D. A. Markelov, M. Dolgushev and E. Lähderanta, in *Annual Reports on NMR Spectroscopy*, ed. G. A. Webb, Academic Press, 2017, vol. 91, pp. 1–66.
53 A. N. Shishkin, D. A. Markelov and V. V. Matveev, Molecular dynamics simulation of poly(butyl)carbosilane dendrimer melts at 600 K, *Russ. Chem. Bull.*, 2016, **65**, 67–74.

Electronic Supplementary Information: Mechanical relaxation of functionalized carbosilane dendrimer melts

Nadezhda N. Sheveleva,[1,2]* Maxim Dolgushev,[3†] Erkki Lähderanta,[2]

Denis A. Markelov[1]

[1]*St. Petersburg State University, 7/9 Universitetskaya nab., St. Petersburg, 199034 Russia.*

[2]*Department of Physics, LUT University, Box 20, 53851 Lappeenranta, Finland.*

[3]*Sorbonne Université, CNRS, Laboratoire de Physique Théorique de la Matière Condensée, LPTMC, 4 place Jussieu, 75005 Paris, France.*

*n.n.sheveleva@spbu.ru, †maxim.dolgushev@sorbonne-universite.fr

This electronic supplementary information contains the details about the molecular dynamics simulations of melts of functionalized dendrimers considered in this study and about the method used for the calculation of their mechanical relaxation moduli.

The mechanical relaxation is studied by adapting the method used in Ref.[1] Here we recall it briefly and provide the information that specific for this study. This method allows overcoming the difficulty of covering a huge region of time scales inherent for the mechanical relaxation. The main feature of the method is the superposition of relaxation curves obtained for dynamical systems subjected to different internal frictions. The dynamics is studied by molecular dynamics simulations performed in the GROMACS package.[2] The dendrimers are modeled in the united atoms framework within Gromos53a6 force-field[3] and placed in the periodic boxes containing 27 macromolecules each. This force-field gives densities of carbosilane dendrimer melts that are very close to the experimental ones.[4,5] At the preliminary stage of equilibration of the systems, V-rescale thermostat of the GROMACS package was used, which was triggered every 0.1 ps, and Berendsen barostat at 1 atm and τ_p = 1 ps. The systems are maintained at the temperature of 600 K by means of the Langevin thermostat in the GROMACS package:

$$m_i \frac{\mathrm{d}^2\vec{r}_i}{\mathrm{d}t^2} = -\frac{m_i}{\tau_T}\frac{\mathrm{d}\vec{r}_i}{\mathrm{d}t} + \vec{F}_i + \vec{w}_i,$$

where m_i and $\vec{r}_i$ are the mass and the coordinate vector of *i*th atom, $\vec{F}_i$ is the external force acting on the *i*th atom, $1/\tau_T$ is the weighted friction constant [1/ps], and $\vec{w}_i$ is a noise process with $\langle w_i(t)w_j(t+s)\rangle = 2(m_i/\tau_T)k_B\mathrm{T}\delta(s)\delta_{ij}$. The Langevin thermostat has been used at different values of the coupling constant τ_T = 0.005, 0.05, 0.5 ps in order to vary the friction in the systems. For the highest value of τ_T, we have simulated ten replicas to have a better statistics at long times. Before using the final trajectories (of 600 ns for G2, 1000 ns for G3, 2000 ns for G4), the systems were equilibrated (in NPT ensemble with Berendsen barostat[6] with 1 atm and thermostat actuation each ps (i.e. τ_p = 1 ps) during 50 ns for G2, 100 ns for G3, 200 ns for G4 and then in NVT ensemble during 100 ns for G2, 200 ns for G3, 600 ns for G4).

The dynamical modulus $G(t)$ is calculated from the fluctuations of the stress tensor $\widehat{\mathbf{P}} = (P_{\alpha\beta})$,[7]

$$G(t) = \frac{V}{30k_{\mathrm{B}}\mathrm{T}}\sum_{(\alpha\beta)}(6\langle P_{\alpha\beta}(t)P_{\alpha\beta}(0)\rangle + \langle N_{\alpha\beta}(t)N_{\alpha\beta}(0)\rangle)$$

Here V is the box volume, T is the temperature, k_B is the Boltzmann constant, $N_{\alpha\beta} = P_{\alpha\alpha} - P_{\beta\beta}$, and the sum runs over components (αβ) = xy, yz, zx of the stress tensor

$$\widehat{\boldsymbol{P}} = \frac{1}{V}\left(\sum_i m_i \vec{v}_i \otimes \vec{v}_i + \sum_{i<j} \vec{r}_{ij} \otimes \vec{F}_{ij}\right)$$

It is calculated in GROMACS based on the microscopic characteristics: the mass m_i and the velocity $\vec{v}_i$ of the united atom group i, the force exerted $\vec{F}_{ij}$ from the group j to i having the distance $|\vec{r}_{ij}|$ between them. The resulting $G(t)$ obtained for different values of the parameter τ_T are superimposed based on the rotational relaxation autocorrelation function,

$$P_1^{rot}(t) = \langle \vec{u}(t) \cdot \vec{u}(0) \rangle,$$

where $\vec{u}(t)$ is the unit vector connecting two silicon atoms, one from the periphery and another one is the core. The exponential tail of the function $P_1^{\text{rot}}(t)$ is characterized through the time τ_{rot} (see Table S1). The $P_1^{\text{rot}}(t)$ related to different τ_T can be perfectly rescaled based on τ_{rot}; the same happens for $G(t)$, see Figure S1. Also we provide the additional parameters of FD and CSD in Table S2.

Table S1. The rotational relaxation time, τ_{rot}, for FD of various generations G for different values of the parameter τ_T characterizing the Langevin thermostat (in ps of GROMACS package).

System	τ_T = 0.005 ps	τ_T = 0.05 ps	τ_T = 0.5 ps
G2	40.528 ns	4.335 ns	0.685 ns
G3	140.622 ns	17.234 ns	2.560 ns
G4	483.914 ns	55.400 ns	8.033 ns

Table S2. The molecular weight, M, the radius of gyration, R_g, and density in the simulation cell for FD and CSD.

System	Density, g/cm^3		M, g/mol		R_g, nm		$D*10^{10}$, m^2/s	
	FD	CSD	FD	CSD	FD	CSD	FD	CSD
G2	0.634	0.669	2131.604	1964.288	0.874	0.872	1.70	1.70
G3	0.634	0.694	4746.252	4241.280	1.141	1.118	0.50	0.54
G4	0.641	0.667	9973.832	8763.008	1.441	1.394	0.18	0.14

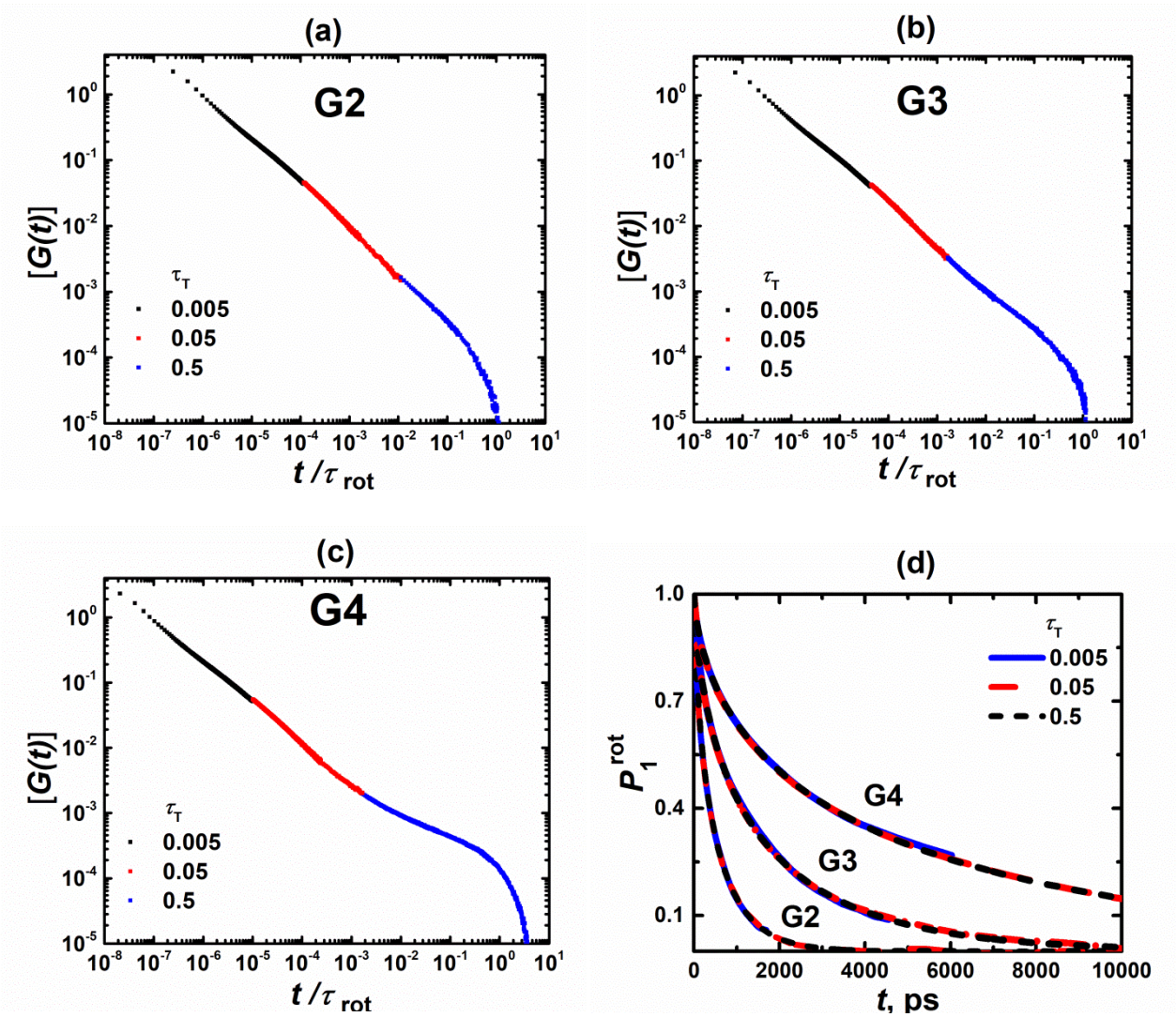

Figure S1. (a)-(c) Normalized shear-stress relaxation modulus $[G(t)] \equiv G(t)/G(0)$ for a melt of FD (G2, G3, and G4, respectively), calculated from simulations employing the Langevin thermostat with different values of the parameter τ_T. The curves are rescaled with τ_{rot} (Table S1) that are obtained from (d) the rotational autocorrelation function $P_1^{\text{rot}}(t)$.

References

1 M. Dolgushev, D. A. Markelov and E. Lähderanta, Linear Viscoelasticity of Carbosilane Dendrimer Melts, *Macromolecules*, 2019, **52**, 2542–2547.

2 M. J. Abraham, T. Murtola, R. Schulz, S. Páll, J. C. Smith, B. Hess and E. Lindahl, GROMACS: High performance molecular simulations through multi-level parallelism from laptops to supercomputers, *SoftwareX*, 2015, **1–2**, 19–25.

3 C. Oostenbrink, A. Villa, A. E. Mark and W. F. Van Gunsteren, A biomolecular force field based on the free enthalpy of hydration and solvation: The GROMOS force-field parameter sets 53A5 and 53A6, *J. Comput. Chem.*, 2004, **25**, 1656–1676.

4 N. K. Balabaev, M. A. Mazo and E. Y. Kramarenko, Insight into the Structure of Polybutylcarbosilane Dendrimer Melts via Extensive Molecular Dynamics Simulations, *Macromolecules*, 2017, **50**, 432–445.

5 A. N. Shishkin, D. A. Markelov and V. V. Matveev, Molecular dynamics simulation of poly(butyl)carbosilane dendrimer melts at 600 K, *Russ. Chem. Bull.*, 2016, **65**, 67–74.

6 H. J. C. Berendsen, J. P. M. Postma, W. F. van Gunsteren, A. DiNola and J. R. Haak, Molecular dynamics with coupling to an external bath, *J. Chem. Phys.*, 1984, **81**, 3684–3690.

7 J. Ramírez, S. K. Sukumaran, B. Vorselaars and A. E. Likhtman, Efficient on the fly calculation of time correlation functions in computer simulations, *J. Chem. Phys.*, 2010, **133**, 154103.